



AMEGHINIANA

A GONDWANAN PALEONTOLOGICAL JOURNAL



This file is an uncorrected accepted manuscript (i.e., postprint). Please be aware that during the production process this version will definitively change. This postprint will be removed once the paper is officially published.

All legal disclaimers that apply to the journal pertain.

Submitted: 10 July 2022 – **Accepted:** 7 February 2023 – **Posted online:** 10 February 2023

To link and cite this article:

doi: 10.5710/AMGH.07.02.2023.3530

PLEASE SCROLL DOWN FOR ARTICLE

1 **LATE PALEOCENE TO MIDDLE EOCENE CALCAREOUS NANNOFOSSIL**
2 **ASSEMBLAGES FROM PENÍNSULA MITRE, SOUTHEASTERN AUSTRAL**
3 **BASIN, ARGENTINA**

4 ASOCIACIONES DE NANOFÓSILES CALCÁREOS DEL PALEOCENO TARDÍO
5 AL EOCENO MEDIO DE PENÍNSULA MITRE, SUDESTE DE LA CUENCA
6 AUSTRAL, ARGENTINA

7

8 ERIKA L. BEDOYA AGUDELO¹, JUAN PABLO PÉREZ PÁNERA², ANDREA
9 CONCHEYRO^{3,4}, EDUARDO OLIVERO^{1,5}, CECILIA GUTIÉRREZ¹, PABLO J.
10 TORRES CARBONELL¹.

11

12 ¹ Centro Austral de Investigaciones Científicas (CADIC-CONICET), Bernardo Houssay
13 200, 9410 Ushuaia, Argentina. erikal.bedoya@gmail.com,
14 torrescarbonell@conicet.gov.ar, cecinesg.21@gmail.com

15 ² CONICET- División Geología, Museo de La Plata, Paseo del Bosque s/n, B1900FWA,
16 La Plata, Argentina. perezpanera@gmail.com

17 ³ Instituto de Estudios Andinos Don Pablo Groeber, Facultad de Ciencias Exactas y
18 Naturales, Universidad de Buenos Aires, Intendente Güiraldes 2160, Ciudad
19 Universitaria, C1428EGA CABA, Buenos Aires, Argentina. aconcheyro@gmail.com

20 ⁴ Instituto Antártico Argentino, 25 de mayo 1143, San Martín, Provincia de Buenos
21 Aires, Argentina.

22 ⁵ Universidad Nacional de Tierra del Fuego (UNTDF), Instituto de Ciencias Polares y
23 Antárticas, Fuegia Basket 251, CP 9410 Ushuaia, Tierra del Fuego, Argentina.
24 emolivero@gmail.com

25

26 30 pag. (text + references); 7 figs.; 1 table

27

28 Running Header: BEDOYA *ET AL.*: PALEOGENE CALCAREOUS NANNOFOSSILS

29 FROM SE AUSTRAL BASIN.

30 Short Description: The Río Claro Group and the Río Bueno Formation biostratigraphy

31 based on calcareous nannofossils, Southeast Isla Grande de Tierra del Fuego, Austral

32 Basin, Argentina.

33

34 Corresponding author: Erika Lorena Bedoya Agudelo erikal.bedoya@gmail.com

35 **Abstract.** On the Fueguian Atlantic coast and in the southern Andean fold and thrust
36 belt, the Paleogene is partially represented by numerous turbiditic deposits. Between
37 Río Bueno and Cabo Leticia in Península Mitre, the Paleocene-Eocene is represented by
38 the Río Claro Group (Cabo Leticia, La Barca, Punta Noguera, and Cerro Ruperto
39 formations) and the Río Bueno Formation; which together constitute a ~1050 m
40 thickness succession. Calcareous nannofossil assemblages recovered from 95 samples
41 were analyzed to determine their relative ages. The Cabo Leticia Formation was barren
42 in nannofossils. The upper LB2 Member of La Barca Formation contained *Rhomboaster*
43 *cuspis* and *Fasciculithus richardii*, frequent in the Paleocene/Eocene boundary
44 (Subzones NP9a/NP9b). Nannofossils recovered from Punta Noguera Formation
45 indicate an early Eocene age (biozones NP9b–NP10), with *Fasciculithus tympaniformis*,
46 *Rhomboaster cuspis*, and abundant *Toweius* spp. The Cerro Ruperto Formation
47 provided one productive sample, with specimens of *Reticulofenestra* spp. and *Toweius*
48 spp., which indicates an early Eocene age for the formation (biozones NP12–NP13).
49 The Río Bueno Formation yields calcareous nannofossil assemblages characterized by
50 *Chiasmolithus eograndis*, *Chiasmolithus expansus*, *Toweius* spp. and *Reticulofenestra*
51 spp. which indicate a late early Eocene to middle Eocene age (biozones NP14–NP16).
52 Although the calcareous nannofossil record is discontinuous due to preservational
53 biases in the Río Claro Group, our data allow a better age constraint for the investigated
54 formations and to correlate these units with other surface and subsurface units in the
55 Austral Basin.

56 **Keywords.** Paleogene. Austral Basin. Calcareous nannofossils. Early Eocene. Tierra del
57 Fuego.

58 **Resumen.** ASOCIACIONES DE NANOFÓSILES CALCÁREOS DEL PALEOCENO
59 TARDÍO AL EOCENO MEDIO DE PENÍNSULA MITRE, SUDESTE DE LA

60 CUENCA AUSTRAL, ARGENTINA. En la costa atlántica fueguina y en la faja
61 plegada y corrida de los Andes Fueguinos, el Paleógeno está representado parcialmente
62 por numerosos sistemas turbidíticos. Entre el Río Bueno y el Cabo Leticia en Península
63 Mitre, el Paleoceno-Eoceno está integrado por la Formación Río Bueno y al Grupo Río
64 Claro (formaciones Cabo Leticia, La Barca, Punta Noguera y Cerro Ruperto) que
65 alcanzan ~1050 m de espesor. En este trabajo se analizan los ensambles de nanofósiles
66 calcáreos de 95 muestras a fin de precisar sus edades relativas. La Formación Cabo
67 Leticia resultó estéril en nanofósiles. El miembro superior de la Formación La Barca,
68 LB2, contiene ejemplares de *Rhomboaster cuspis* y *Fasciculithus richardii*, frecuentes
69 en el límite Paleoceno/Eoceno (Subzonas NP9a–NP9b). Los nanofósiles recuperados en
70 la Formación Punta Noguera indican una edad Eoceno temprano (subzonas NP9b–
71 NP10), con *Fasciculithus tympaniformis*, *Rhomboaster cuspis* y abundantes *Toweius*
72 spp. La Formación Cerro Ruperto proporcionó una muestra fértil, con ejemplares de
73 *Reticulofenestra* spp. y *Toweius* spp., asignables al Eoceno temprano (biozonas NP12–
74 NP13). La Formación Río Bueno, proveyó *Chiasmolithus eograndis*, *Chiasmolithus*
75 *expansus* *Toweius* spp. y *Reticulofenestra* spp. Asignables al Eoceno temprano tardío -
76 Eoceno medio (biozonas NP14–NP15).

77 Aunque el registro de nanofósiles calcáreos es discontinuo debido a las facies
78 sedimentarias del Grupo Río Claro, nuestros datos permiten una mejor restricción de la
79 edad de las formaciones investigadas y correlacionarlas con otras unidades aflorantes y
80 del subsuelo en la Cuenca Austral.

81 **Palabras clave.** Paleógeno. Cuenca Austral. Nanofósiles calcáreos. Eoceno Temprano.
82 Tierra del Fuego.

83 THE SOUTHERNMOST PORTION of the South American Andean Cordillera ends in the
84 Fuegian Andes. Here, the Fuegian Thrust-Fold Belt includes foreland basin successions
85 from the Upper Cretaceous to the Miocene (Olivero *et al.*, 2002, 2003; Torres Carbonell
86 *et al.*, 2011; Torres Carbonell & Olivero, 2019). This work focuses on the stratigraphic
87 record along the Atlantic shore of Península Mitre, SE Tierra del Fuego (Fig. 1.1),
88 where a complex marine sedimentary succession from the Upper Cretaceous–Danian
89 (Policarpo Formation) to the Paleogene (Río Claro Group and Río Bueno Formation)
90 are exposed (Fig. 1.2).

91 The integrated stratigraphy of Paleogene rocks in the study area was based on
92 dinocysts, foraminifera, and calcareous nannofossil assemblages. Accordingly, an upper
93 Paleocene to middle Eocene age was assigned to formations now included in the Río
94 Claro Group and middle Eocene for the Río Bueno Formation (Olivero *et al.*, 2002;
95 Malumián & Jannou, 2010; Bedoya Agudelo, 2019).

96 Detailed calcareous nannofossil biostratigraphic studies have been done in
97 subsurface successions of the northern Isla Grande de Tierra del Fuego and southeast
98 Santa Cruz Province (*e.g.*, Mostajo, 1991; Pérez Panera 2009, 2013; Thissen & Pérez
99 Panera, 2021). These studies prove the usefulness of calcareous nannofossils for relative
100 age determination, and intrabasinal correlation in the Austral Basin. Despite the
101 excellent exposures of Paleogene units at the southern Isla Grande de Tierra del Fuego,
102 their calcareous nannofossil record remain relatively unknown (*e.g.*, Pérez Panera *et al.*,
103 2017; Bedoya Agudelo *et al.*, 2018; Bedoya Agudelo, 2019). Here we present new field
104 data and interpretations, which allow better constraints on the depositional age of the
105 Río Claro Group and Río Bueno Formation and the timing of some important tectonic
106 events in this part of the Austral Basin (*e.g.*, correlation between angular
107 unconformities).

108 Based on the calcareous nannofossils assemblages and their stratigraphic
109 relationship, this paper aims to 1) revise the relative ages of the different formations that
110 integrate the Río Claro Group and the Río Bueno Formation; and 2) to correlate these
111 units with the subsurface units. It should be noted that in some formations, the
112 nannofossil are scarce due to the turbidite facies that conform to the Río Claro Group.
113 Moreover, the outcrops in this remote area are restricted to the coastal cliffs and inland
114 river valleys of difficult access, limiting sampling to discontinuous stratigraphic
115 columns. However, we were able to cover the fine-grained siliciclastic and calcareous
116 facies present in each formation leading to an improved biostratigraphic framework.

117 **Institutional abbreviations.** CADIC-CONICET, Centro Austral de Investigaciones
118 Científicas Ushuaia–Consejo Nacional de Investigaciones Científicas y Tecnológicas,
119 Ushuaia, Argentina.

120 **GEOLOGICAL SETTING**

121 The Paleogene of Península Mitre is represented by a set of formations (Fig. 2)
122 exposed along the Fuegian Atlantic coast, between the Río Bueno area and the Cabo
123 Irigoyen (Fig. 1.2) (Olivero *et al.*, 2002, 2003, 2007; Olivero & Malumián, 2008). Part
124 of the Paleogene succession, grouped into the Río Claro Group and the Río Bueno
125 Formation represent a regressive megasequence, starting with turbidite deposits towards
126 the base and prograding into shallower facies (Olivero & Malumián, 2008). The
127 stratigraphic framework of the studied area is briefly described, based on the
128 generalized section shown in Figure 3.1.

129 Figure 1.

130 **Río Claro Group**

131 In the studied area, the Río Claro Group comprises the Cabo Leticia, La Barca,
132 Punta Noguera, and Cerro Ruperto formations (Olivero & Malumián, 2008).

133 **Cabo Leticia Formation.** The oldest unit of the Group, crops out in its type locality
134 (Cabo Leticia) at the core of an asymmetrical anticline, where it reaches 150 m of
135 thickness (Olivero *et al.*, 2002) and at Río Malengüena (Torres Carbonell *et al.*, 2011).
136 The Cabo Leticia Formation is composed of breccias, conglomerates with abundant
137 fragments of poorly preserved oyster shells, and tuffaceous sandstones interpreted as
138 gravity flows, deposited in a fan delta environment (Olivero *et al.*, 2002). The base of
139 the formation is not exposed and the top is transitional with the La Barca Formation
140 (Olivero *et al.*, 2002).

141 Figure 2.

142 **La Barca Formation.** The type area of the La Barca Formation is located between the
143 Cabo Leticia and playa La Barca, where it reaches a minimum thickness of 220 m
144 (Olivero *et al.*, 2002). The Formation includes two members, the LB1 member (Fig.
145 3.1–3.3), with a minimum exposed thickness of 120 m, and the LB2 member (Fig. 3.2),
146 approximately 100 m thick (Olivero *et al.*, 2002). In the Río Malengüena area, the
147 formation crops out to the north and south of Punta Ainol, where it is deformed by an
148 anticline-syncline pair.

149 To the south, the top of this unity is in tectonic contact with the Leticia
150 Formation (middle–upper Eocene) through a reverse fault. To the north, the La Barca
151 Formation is unconformably covered by the Leticia Formation (Torres Carbonell *et al.*,
152 2011).

153 The La Barca Formation is characterized by interbedded tuffaceous sandstones
154 and carbonaceous siltstones (member LB1) and by black to dark gray mudstones with
155 levels of ellipsoidal concretions that reach up to 2.5 m in their long axis (member LB2).
156 These facies are interpreted as anoxic marine deposits (Olivero & Malumián, 2008;
157 Torres Carbonell *et al.*, 2009). The presence of agglutinated foraminifera such as

158 *Spiroplectammina spectabilis* and endemic species such as *Buliminella isabelleana*
159 *procera* and *Antarcticella* sp., allowed assigning a late Paleocene age (Malumián &
160 Jannou, 2010). Recent evidence based on calcareous nannofossils (Bedoya Agudelo *et*
161 *al.*, 2018) and dinocyst assemblages (Quattrocchio, 2021) also record lower Eocene
162 horizons.

163 **Punta Noguera Formation.** The type section of the Punta Noguera Formation is
164 exposed at the core of a syncline fold in the Punta Noguera area, with a minimum
165 thickness of 380 m (Fig. 3.1) (Olivero *et al.*, 2002). To the west, at Punta Ainol and at
166 the Río Malengüena area, the strata of this unit are overturned (Torres Carbonell *et al.*,
167 2011).

168 This formation is characterized by rhythmically stratified massive glauconitic
169 sandstones, dark mudstones, and fine conglomerates, interpreted as turbidites (Olivero
170 & Malumián, 2008) deposited at the foot of fan-deltas (Olivero *et al.*, 2002). The
171 thickest sand-rich turbidite beds bear abundant fragments of molluscan shells (Fig. 3.1).
172 At Punta Ainol, the formation is composed of fine sandstones with high content of
173 volcanoclastic material, interspersed with levels of sandstones with heterolithic
174 stratification (Torres Carbonell *et al.*, 2009). These sediments contain ostracods,
175 radiolaria, and agglutinated foraminifera of the genera *Rzehakina*, *Criborotalia*,
176 *Elphidium* (Malumián & Jannou, 2010), and the species *Chiloguembelina wilcoxensis*,
177 constraining the age to the early Eocene (Malumián *et al.*, 2009; Torres Carbonell *et al.*,
178 2009). At Punta Ainol, the base and top of this unit are covered, whilst at Punta
179 Noguera, the top is unconformably covered by the Río Bueno Formation (Furque &
180 Camacho, 1949; Olivero *et al.*, 2002).

181 Figure 3.

182 **Cerro Ruperto Formation.** The type section of the Cerro Ruperto Formation crops out
183 between Punta Cuchillo and Cerro Ruperto, with a minimum, exposed thickness of 200
184 m (Olivero *et al.*, 2002). The Cerro Ruperto Formation comprises glauconite-rich
185 sandstones and siltstones, deposited in a restricted marine environment (Olivero &
186 Malumián, 2008). It contains abundant solitary corals, gastropods, bivalves, radiolaria,
187 and well-preserved dinocysts, like *Deflandrea dartmooria* from the early Eocene
188 (Olivero *et al.*, 2002). The base is not exposed and the top is unconformably covered by
189 the Río Bueno Formation (Olivero *et al.*, 2002).

190 **Río Bueno Formation**

191 The Río Bueno Formation (Furque & Camacho, 1949; Olivero *et al.*, 2002) is
192 formed by two members, RB1 and RB2, which crop out in different localities. RB1 is
193 exposed at Punta Noguera (the type section), Cerro Las Vacas, the northern coast of the
194 Laguna Río Bueno, and Meseta de Orozco, with a minimum thickness of 30–40 m. The
195 member RB2 crops out at the intertidal zone near Puesto Río Bueno, with a similar
196 thickness. The Río Bueno Formation is composed of calcareous rocks with two
197 lithological associations; RB1, formed by bioclastic limestones (mainly grainstones),
198 and RB2 formed by an alternation of limestones, bioturbated marls, and micrites, all
199 deposited in a shallow platform environment (Olivero *et al.*, 2002; Torres Carbonell,
200 2010). These sediments contain abundant fossils constrained to the lower middle
201 Eocene, such as fragments of bivalves, gastropods, solitary corals, bryozoans, and
202 calcareous algae, as well as radiolaria, ostracods and benthic and planktonic
203 foraminifera (*Planorotalites australiformis* and *Subbotina linaperta*) (Olivero *et al.*,
204 2002). The base of the formation covers in angular unconformity several units of
205 different ages, from the Maastrichtian to the Paleocene, and to the lower Eocene such as

206 the Policarpo, Cabo Leticia, La Barca, Punta Noguera and Cerro Ruperto formations,
207 while the top is not exposed.

208 Previous structural and stratigraphic work in the area labelled this unconformity
209 as U3, and related it to significant exhumation related to a stage of Paleocene–early
210 Eocene thrusting and folding in this part of the thrust-fold belt (Olivero *et al.*, 2002;
211 Torres Carbonell *et al.*, 2011; 2020). Deposition of the Río Bueno Formation atop this
212 unconformity indicates that it forms part of a wedge-top depocenter within the foreland
213 basin system (Torres Carbonell & Olivero, 2019). Our new data regarding the age of the
214 Río Bueno Formation gives a better constraint of the youngest age of this deformation
215 stage and initiation of the wedge-top depocenter.

216 The analyzed samples in this study comprise both members of the Río Bueno
217 Formation. Because the RB1 and RB2 members are not in contact, their stratigraphic
218 relationships are uncertain. Olivero *et al.* (2002) tentatively assumed that member RB2
219 overlies the member RB1; however, as the microfossil content is not conclusive, the
220 opposite alternative is also possible.

221 **MATERIALS AND METHODS**

222 **Materials**

223 A total of 95 samples collected in several field seasons by EBO, PTC and CG,
224 were processed and analyzed for calcareous nannofossils. These were collected in
225 several localities (Fig. 1.2) of Península Mitre: Río Leticia, Laguna Río Bueno, Punta
226 Noguera, Cerro Ruperto, Río Malengüena, Punta Ainol, and Punta Cuchillo. They
227 represent partial sections totalizing 1050 m thick-composite sections and are compiled
228 on a single composite stratigraphic section (Fig. 3).

229 The recovered material and nannofossil fertile slides are stored in the
230 Micropaleontological Collection Repository of CADIC–CONICET, under the acronym

231 CADIC MIC- (Cadic Micropaleontología) (Tab. 1). Barren samples keep the field code
232 under which they were collected.

233 Table 1.

234 **Methods**

235 The samples were prepared following the smear slide standard technique (Bown
236 and Young, 1998). Nannofossils were observed using a polarized light Leica DM750
237 microscope under 1000x magnification. Semiquantitative analysis was performed, and
238 counts of 300 specimens were made along random longitudinal transects in the slides.
239 In samples with low abundance, the total nannofossils observed in 10 longitudinal
240 transects were counted. Relative species abundances were estimated as follows: VA=
241 very abundant (>10 specimens/field of view); A = abundant (1–9 specimens/field of
242 view); C = common (1 specimen/2–10 fields of view) F = few (1 specimen/11–50 fields
243 of view); R = rare (1 specimen/ > 50 fields of view); B = barren. The preservation was
244 estimated by examining the qualitative degree of dissolution and/or recrystallization:
245 good (G), for specimens with little or no evidence of dissolution and/or overgrowth;
246 moderate (M), for specimens with little or some dissolution and/or overgrowth, but that
247 are still identifiable; and poor (P), for specimens with considerable dissolution and/or
248 recrystallization.

249 Taxonomic concepts for species follow Perch-Nielsen (1985), Bown (2005,
250 2016) and the online Nannotax Catalog (Young *et al.*, 2022). The standard zonation
251 scheme of Martini (1971) for the Cenozoic was used as a reference.

252 **RESULTS**

253 Recovered nannofossil assemblages in the Río Claro Group and Río Bueno
254 Formation show highly variable preservation and abundance. All calcareous nannofossil

255 species recovered in the studied formations are summarized in Figure 4. Most
256 representative species are illustrated in Figures 5 and 6.

257 Figure 4.

258 **Cabo Leticia Formation**

259 Two samples from the Cabo Leticia Formation, one from Cabo Leticia locality
260 and the other from the Río Malengüena, were barren in calcareous nannofossils.

261 **La Barca Formation**

262 In the analyzed samples from the LB1 and LB2 members of the La Barca
263 Formation in Cabo Leticia, calcareous nannofossils were not recorded. Only a single
264 specimen of *Hornibrookina australis* in sample 372-21 of the member LB2 was
265 recognized. In samples from the Río Malengüena, mainly composed of black
266 mudstones, calcareous nannofossils were also not recognized (Fig. 3.3).

267 Figures 5 and 6.

268 From the Punta Ainol section, 16 samples of the LB2 member were fertile (Fig.
269 3.2). The abundance was low to moderate throughout the section. The preservation is
270 mostly poor, and species richness is low to moderate.

271 In the lower part of the profile (samples CADIC MIC-01 to CADIC MIC-08),
272 assemblages show low abundance and poor to moderate preservation. They are
273 characterized by small placoliths like *Toweius occultatus*, *Toweius eminens*, and
274 *Toweius rotundus*, with few to rare *Chiasmolithus bidens*, *Coccolithus pelagicus*, and
275 *Fasciculithus involutus*. Other late Paleogene important species recovered in this lower
276 part are *Fasciculithus alanii*, *Fasciculithus mitreus*, *Fasciculithus richardii*, and
277 *Fasciculithus tympaniformis*, see Supplementary Online Information (SOI).

278 In the upper part (samples CADIC MIC-09 to CADIC MIC-16), assemblages
279 have poor preservation. However, these assemblages have high species richness and

280 show an increase in the relative abundance of the genus *Toweius*, and *Chiasmolithus*
281 *bidens* and *Coccolithus pelagicus*.

282 In the lower sample of this part (CADIC MIC-09) (see SOI) the species richness
283 is higher compared to the other samples, and some events close to the Paleocene/Eocene
284 boundary were identified, like the Last Occurrence (**LO**) of *F. alanii* and LO of *F.*
285 *richardii*, and the First Occurrence (**FO**) of *C. solitus*, *Discoaster* cf. *araneus* and *R.*
286 *cuspis*.

287 In addition, specimens of the genus *Heliolithus* (*H. kleinpellii* and *H. cantabriae*)
288 and *Watznaueria* sp., observed both, in the lower and the upper part of the profile are
289 considered as reworked taxa.

290 **Punta Noguera Formation**

291 At its type section, the recovered calcareous nannofossils exhibit poor
292 preservation, low abundance, and medium to high species richness. Some samples were
293 barren. Species richness decreases towards the upper levels, whereas abundance slightly
294 increases.

295 Assemblages are characterized by high relative abundance of *Chiasmolithus*
296 *bidens*, *Coccolithus pelagicus*, *Toweius callosus*, and *Toweius occultatus*. The presence
297 of *Chiasmolithus solitus*, *Chiasmolithus eograndis*, *Cyclicarcolithus parvus*,
298 *Fasciculitus tympaniformis*, *Fasciculithus involutus*, *Fasciculithus* cf. *sidereus*,
299 *Hornibrookina australis*, cf. *Rhomboaster cuspis*, and the LOs of *Prinsius bisulcus* and
300 *Prinsius martini* (see SOI) indicate an early Eocene age.

301 **Cerro Ruperto Formation**

302 In the studied section of the Cerro Ruperto Formation, only one sample yields
303 calcareous nannofossils (sample CADIC MIC-170; see SOI). This assemblage has
304 moderate preservation and moderate abundance and species richness. It is characterized

305 by *Blackites creber*, *Chiasmolithus* spp., *Coccolithus formosus*, *Coccolithus* spp.,
306 *Coronocyclus bramlettei*, *Ellipsolithus bollii*, *Helicosphaera* sp., *Neococcolithes dubius*,
307 *Pontosphaera pectinata*, *Pontosphaera pulchra*, *Reticulofenestra* spp., *Toweius* spp.,
308 and *Umbilicosphaera* sp. In this sample *Reticulofenestra dictyoda* and small specimens
309 of *Reticulofenestra* spp. are the most abundant taxa, followed by *Chiasmolithus solitus*,
310 *Coccolithus pelagicus*, *R. lockeri*, and unidentified species of the genus *Toweius* and
311 *Umbilicosphaera* (see SOI). The presence of *Coccolithus formosus*, *Neococcolithes*
312 *dubius*, and the high relative abundance of *Reticulofenestra* spp. and *Toweius* spp.,
313 indicates an early Eocene age for this assemblage.

314 **Río Bueno Formation**

315 The 16 investigated samples of the Río Bueno Formation covered the two
316 members of this formation. For the lower RB1 Member, 11 samples (Figs. 3.1, SOI)
317 were taken from different sections in the intertidal area of the Punta Noguera type
318 section. For the RB2 member, five samples (Figs. 3.1, SOI) were taken from different
319 points near the Puesto Río Bueno and the Río Leticia (Fig. 1.2).

320 In member RB1, nannofossil assemblages display few abundance, and moderate
321 preservation and species richness. The assemblage is characterized by *Coccolithus*
322 *pelagicus*, *Toweius callosus*, and *Toweius* spp. reworking from the earliest Eocene is
323 recognized by the presence of *Ellipsolithus bollii*, *Hornibrookina arca*, *Neochiastozygus*
324 *junctus* and *Toweius occultatus*. However, some common species from the middle
325 Eocene as *Chiasmolithus grandis*, *Chiasmolithus expansus*, *Neococcolithes minutus*, and
326 *Reticulofenestra wadeae* could be identified (see SOI).

327 In the RB2 member there is a decrease in nannofossil abundance, together with a
328 poor preservation. Only one sample (CADIC MIC-174) contains calcareous
329 nannofossils. The assemblage is dominated by *Coccolithus pelagicus*, followed by

330 *Toweius callosus*. Rare taxa include *H. arca*, *N. junctus*, *P. pulchra*, *Reticulofenestra*
331 spp., *S. moriformis*, *Toweius* spp., and *Z. bijugatus* (see SOI).

332 **DISCUSSION**

333 The Río Claro Group and Río Bueno Formation correspond to lower Paleogene
334 turbidite deposits (Olivero & Malumián, 2008), thus microfossil recovery is patchy and
335 biased by siliciclastic dilution. However, calcareous nannofossil results from the
336 investigated sections allow a better age constraint for these successions and correlation
337 with subsurface units (Fig. 7).

338 At the lower part of the Río Claro Group, the Cabo Leticia Formation is barren
339 in calcareous nannofossils. However, an late Paleocene age is considered herein,
340 following Olivero *et al.* (2002) based on stratigraphic relationships with the overlying
341 La Barca Formation (upper Paleocene-lower Eocene) (Bedoya Agudelo *et al.*, 2018).

342 The La Barca Formation comprises the upper Paleocene- lower Eocene based on
343 the FOs of *Discoaster* cf. *araneus* and *Rhomboaster cuspis*, and the LOs of *F. alanii*
344 and *Fasciculithus richardii* group (*F. richardii*, *F. mitreus*, sensu Agnini *et al.*, 2014).
345 These events were recorded on samples of the member LB2 in the Punta Ainol area and
346 constrain the assemblage to the NP9a/NP9b subzones (s. Agnini *et al.*, 2007) (Bedoya
347 Agudelo *et al.*, 2018). This subzonal boundary indicates the Paleocene/Eocene
348 boundary (56 Ma, Speijer *et al.*, 2020). The presence of the genus *Rhomboaster* in the
349 sample CADIC MIC-09 and *Fasciculithus tympaniformis* in samples CADIC MIC-09 to
350 CADIC MIC-16 representing NP9b–NP10 biozones of Martini (1971), would indicate a
351 lower Eocene age for the upper part of the LB2 Member.

352 Analyzed samples of the LB1 Member, (La Barca Formation) in this study were
353 barren, possibly due to the lithology, characterized by volcaniclastic sandstones
354 (Olivero *et al.*, 2002). According to Malumián and Caramés (2002), the LB1 Member

355 would correspond to facies accumulated in low oxygen due to high paleoproductivity
356 and organic matter accumulation, which could explain the absence of calcareous
357 microfossils (nannofossils and planktic foraminifera) due to high concentration of
358 carbon dioxide and calcium carbonate dissolution.

359 Figure 7.

360 The La Barca Formation was originally assigned to the upper Paleocene due to
361 the presence of *Bulimina karpatica* Szczechura (Malumián & Caramés, 2002),
362 *Palaeocystodinium golzowense* Alberti, and *Glaphyrocysta* sp. in the LB1 Member at
363 Cabo Leticia (Olivero *et al.*, 2002). This age was also assigned to the LB2 Member
364 (Malumián & Caramés, 2002; Olivero *et al.*, 2002; Torres Carbonell *et al.*, 2009). Later
365 on, the LB2 Member at Punta Ainol was assigned to the upper Paleocene–lower Eocene,
366 based on calcareous nannofossils and dinocysts assemblages (Bedoya Agudelo *et al.*,
367 2018; Quattrochio, 2021).

368 The late Paleocene and Paleocene/Eocene boundary seems to be absent in
369 subsurface units in the southeastern Santa Cruz Province and northern of Tierra del
370 Fuego Island (Pérez Panera, 2009, 2013; Thissen & Pérez Panera, 2021). Therefore,
371 Punta Ainol is a reference section for this boundary in the Austral Basin.

372 In the Punta Noguera Formation, recovered calcareous nannofossil assemblages
373 are characterized by the presence of *Fasciculithus tympaniformis*, *Fasciculithus*
374 *involutus*, *Fasciculithus* cf. *sidereus*, and *Rhomboaster cuspis*. The genus *Fasciculithus*
375 has its LO in the NP10 Biozone of Martini (1971) and *Rhomboaster cuspis* is restricted
376 to the upper NP9 Biozone and lower NP10 Biozone (Raffi *et al.*, 2005; Agnini *et al.*,
377 2007; Agnini *et al.*, 2014). As there are no evident changes in the calcareous
378 nannofossil assemblages throughout the whole investigated section, we propose an early
379 Eocene age (early Ypresian-NP10 Biozone) for the Punta Noguera Formation. This age

380 is consistent with the interpreted age of the underlying La Barca Formation, which
381 indicate the upper Paleocene–lower Eocene.

382 Most common calcareous nannofossil species in the recovered assemblages are
383 *Chiasmolithus bidens*, *Chiasmolithus solitus*, *Fasciculithus tympaniformis*, *Prinsius*
384 *martini*, *Prinsius bisulcus*, *Toweius callosus*, *Toweius eminens*, and *Toweius pertusus*.
385 This assemblage bears similarities with the Lower Uribe Formation from the subsurface
386 of Tierra del Fuego (Mostajo, 1991; Thissen & Pérez Panera, 2021) and the Lower
387 Magallanes Formation from the subsurface of Santa Cruz province (Pérez Panera, 2013)
388 (Figure 7). It can be also correlated with the nannofossil assemblages from the lower
389 part of the Punta Torcida Formation (Pérez Panera *et al.*, 2017; Bedoya Agudelo, 2019).

390 Regarding the age interpreted by other microfossils, Olivero *et al.* (2002) found
391 a dinocysts association composed of *Apectodinium homomorphum*, *Deflandrea robusta*,
392 and *Palaeocystodinium* sp., suggesting an age close to the Paleocene/Eocene boundary.
393 The foraminifera *Alabama creta* Finlay *Charltonina acutimarginata* Finlay, and the
394 genera *Cribrorotalia* and *Elphidium*, are typical of post-Paleocene shallow waters and
395 close to the Paleocene/Eocene boundary (Olivero *et al.*, 2002), together with
396 *Chiloguembelina wilcoxensis* (Cushman and Ponton), a planktic species of
397 chronostratigraphic value in southern latitudes (Malumián *et al.*, 2009), allowed to
398 assign an early Eocene age. These ages agree with the calcareous nannofossil
399 interpretations.

400 In the Cerro Ruperto Formation, calcareous nannofossil assemblages are
401 characterized by the presence of abundant *Reticulofenestra dictyoda*, *R. lockeri*, *R.*
402 *minuta*, and *Reticulofenestra* spp., together with *Toweius callosus* and *Toweius* spp. The
403 occurrence of the genus *Reticulofenestra* at high latitudes is recognized from Biozone
404 NP11 (Schneider *et al.*, 2011; Shepherd & Kulhanek, 2016). The *Toweius* -

405 *Reticulofenestra* turnover is an important event of the early Eocene, recorded in high
406 and low latitudes around biozones NP12 and NP13 (Martini, 1971; Agnini *et al.*, 2006;
407 Shamrock & Watkins, 2012; Shepherd and Kulhanek, 2016).

408 Considering the presence of both *Reticulofenestra* and *Toweius* characteristic of
409 the NP12–NP13 biozones, in the productive sample from the Cerro Ruperto Formation,
410 we propose a lower Eocene age for the formation, and it is consistent with the
411 interpreted age of the underlying Punta Noguera Formation (lower Eocene). The most
412 distinctive species of the Cerro Ruperto Formation are *C. solitus*, *P. pulchra*, *R.*
413 *dictyoda*, and *R. minuta*, which allow partial correlation with the subsurface Lower
414 Uribe Formation from Tierra del Fuego and the subsurface Lower Magallanes
415 Formation from Santa Cruz province (Mostajo, 1991; Pérez Panera, 2009, 2013) (Fig.
416 7). This assemblage also can be correlated to the nannofossil assemblage and events
417 recorded at Punta Torcida Formation (Pérez Panera *et al.*, 2017; Bedoya Agudelo,
418 2019).

419 Based on the dinocysts *Deflandrea dartmooria* (Williams), the abundant
420 radiolaria *Nodosoria longicasta* d'Orb., and the presence of the foraminifera
421 *Spiroplectamina spectabilis* (Grzybowski), an early Eocene age was assigned for the
422 microfauna of the lower part of the Cerro Ruperto Formation (Olivero *et al.*, 2002),
423 which is in agreement with the calcareous nannofossils age reported here.

424 The reduced samples with nannofossils in the Cerro Ruperto Formation can be
425 related to unfavorable conditions for its fossilization, as well as the deposition in a
426 restricted marine environment (Olivero *et al.*, 2002), massive sandstone facies, and the
427 high abundance of radiolaria which indicates deepening of the basin (Malumián &
428 Jannou, 2010).

429 In the Río Bueno Formation, calcareous nannofossil assemblages are represented
430 by *C. expansus*, *C. eograndis*, *C. solitus*, *N. minutus*, and *R. wadeae*. *Reticulofenestra*
431 *wadeae*, is common in NP14 to NP16 biozones, and *C. expansus*, present in the
432 uppermost productive sample, is common in Biozone NP15 (see SOI). The presence of
433 *Toweius callosus*, *T. occultatus*, and *Chiasmolithus eograndis*, species that are common
434 in the NP14 biozone but also have their last occurrences in that biozone (Shamrock &
435 Watkins, 2012; Shepherd & Kulhanek, 2016), are the most biostratigraphically
436 important components in the Río Bueno assemblages. According to this, the RB1
437 Member of the Río Bueno Formation correlates with NP14–NP15 biozones (the upper
438 part of the early Eocene to the early middle Eocene).

439 *Chiasmolithus bidens*, *Ellipsolithus* sp., *H. arca*, and *N. junctus* were also
440 observed, and are frequently found in the early Eocene (NP10–NP11 biozones), and are
441 considered as reworked material. The limestone deposition of the Río Bueno Formation
442 in Tierra del Fuego occurs after an erosive period, which largely explains the presence
443 of reworked species (Malumián, 1999).

444 The assemblage from the Río Bueno Formation bears similarities with the upper
445 member of the Punta Torcida Formation (Bedoya Agudelo, 2019), the subsurface Lower
446 Uribe Formation from Tierra del Fuego (Mostajo, 1991), and the Lower Magallanes
447 Formation of Santa Cruz province (Pérez Panera, 2013), and the Agua Fresca (Chile),
448 Río Turbio and Man Aike (Santa Cruz) surface formations (Thissen & Pérez Panera,
449 2021).

450 Based on the presence of *Subbotina patagonica*, *Planorotalites australiformis*
451 (Jenkins) and *Subbotina linaperta* (Finlay), a lower middle Eocene age was interpreted
452 for this unit by Olivero *et al.*, (2002) and Malumián and Jannou (2010).

453 Although the Río Bueno Formation assemblages contain reworked taxa from the
454 lowermost Eocene deposits, the age of the formation could not be older than the upper
455 part of the lower Eocene because the Río Bueno Formation lays on an angular
456 unconformity cutting several lower Eocene units (Cerro Ruperto and Punta Noguera
457 formations), which were folded before the development of the unconformity (Olivero *et*
458 *al.*, 2002; Torres Carbonell *et al.*, 2011). It is important to note that abundant specimens
459 of *Reticulofenestra* were not found being part of the nannofossil assemblages of
460 member RB1, taking into account that nannofossil assemblages of the underlying lower
461 Eocene formation (Cerro Ruperto) contain *Reticulofenestra*.

462 Our new data constrains the oldest age of the U3 unconformity to the early
463 Eocene (late Ypresian) since it separates the NP12–NP13 Cerro Ruperto Formation
464 from the NP14–NP15 Río Bueno Formation. This indicates that the significant
465 deformation and erosion of the thrust-fold belt that led to the development of this
466 important angular unconformity has the youngest age within the early Eocene
467 (Ypresian). This data precludes a correlation between U3 and U4 (Fig. 2), which has an
468 age between ca. 46 and 43 Ma and separates the Punta Torcida Formation from the
469 Leticia Formation (Olivero *et al.*, 2020). U4 is also a more regional unconformity, with
470 occurrence beyond the thrust-fold belt, indicating exhumation caused not only by local
471 development of structures, as may be the case of U3 (Torres Carbonell & Olivero,
472 2019). In addition, our data indicate that the initiation of wedge-top deposition in the
473 Austral Basin (with the deposits of the Río Bueno Formation) indicates the late
474 Ypresian age.

475 **Conclusions**

476 In summary, the assemblages recorded in the Río Claro Group and the Río
477 Bueno Formation indicate a late Paleocene-middle Eocene age, correlable to NP9 to
478 NP15 biozones, ~56 to 43 Ma (Speijer *et al.*, 2020).

479 These assemblages allow correlations of these formations with others from
480 drilled sediments previously studied in other sectors of the Austral Basin, like from S-
481 SE of Santa Cruz province and the north-central Tierra del Fuego subsurface, which
482 include broadly NP10 and NP12 to NP15 biozones.

483 Although analyzed samples from Cabo Leticia Formation are barren of
484 calcareous nannofossils, it is most probable that this formation represents a late
485 Paleocene sedimentation due to its stratigraphic position.

486 The LB2 Member of the La Barca Formation at Punta Ainol indicates an upper
487 Paleocene–lower Eocene, equivalent to the NP9a/NP9b subzones, defined by the
488 presence of *Fasciculithus alanii*, *Fasciculithus richardii* and *Rhomboaster cuspis*. In
489 other sectors of the basin, the late Paleocene and the earliest Eocene are represented by
490 hiatuses, making the La Barca Formation in the Punta Ainol area a reference section for
491 this interval in the Austral Basin.

492 The Punta Noguera Formation is confirmed to be lower Eocene (early Ypresian,
493 NP10 Biozone), due to the presence of *Fasciculithus tympaniformis*, *Fasciculithus*
494 *involutus* and the absence of *Reticulofenestra* spp.

495 The calcareous nannofossils assemblage found in the Cerro Ruperto Formation
496 is composed of *C. solitus*, *Coccolithus* cf. *crassus*, *C. latus*, *E. formosa*, *N. dubius*, *R.*
497 *dictyoda*, *R. lockeri*, *R. minuta*, and *T. callosus*, allow us to assign an early Eocene age,
498 equivalent to biozones NP12–NP13.

499 In the Río Bueno Formation, the recorded assemblage is mostly reworked;
500 however, some species such as *C. expansus*, *N. minutus*, and *R. wadeae* allow assigning

501 an age not younger than the middle Eocene, equivalent to NP14–NP15 biozones. The
502 U3 unconformity below the Río Bueno Formation thus represents the lower Eocene
503 (upper Ypresian) and marks the onset of the wedge-top depocenter in the foreland basin
504 during that age.

505 This age also precludes the correlation of U3 with the younger and more regional U4
506 unconformity.

507 **ACKNOWLEDGMENTS**

508 We thank Daniel Martinioni and Facundo Fuentes for their help during some of the
509 fieldwork seasons. This manuscript was improved for the constructive corrections and
510 suggestions made by Clever Alves (Fundação Coppetec, Brasil), and José Cuitiño
511 (CONICET, Argentina), and the Ameghiniana Editorial Committee. The results are part
512 of the postdoctoral research program in progress of ELBA (CADIC-CONICET),
513 supported by project PIDUNTdF-A1. This is the contribution R-433 of the Instituto de
514 Estudios Andinos “Don Pablo Groeber”.

515 **REFERENCES**

- 516 Agnini, C., Fornaciari, E., Raffi, I., Catanzariti, R., Pälke, H., Backman, J., & Rio, D.
517 (2014). Biozonation and biochronology of Paleogene calcareous nannofossils from
518 low and middle latitudes. *Newsletters on Stratigraphy*, 47(2), 131–181.
- 519 Agnini, C., Fornaciari, E., Rio, D., Tateo, F., Backman, J., & Giusberti, L. (2007).
520 Responses of calcareous nannofossil assemblages, mineralogy, and geochemistry to
521 the environmental perturbations across the Paleocene/Eocene boundary in the
522 Venetian Pre-Alps. *Marine Micropaleontology*, 63(1–2), 19–38.
- 523 Agnini, C., Muttoni, G., Kent, D. V., & Rio, D. (2006). Eocene biostratigraphy and
524 magnetic stratigraphy from Possagno, Italy: The calcareous nannofossil response to
525 climate variability. *Earth and Planetary Science Letters*, 241(3–4), 815–830.

526 Bedoya Agudelo, E. L. (2019). *Asociaciones de nanofósiles calcáreos del Paleoceno-*
527 *Mioceno de Tierra del Fuego. Bioestratigrafía y paleoecología.* (Tesis Doctoral,
528 Facultad de Ciencias Exactas y Naturales, Universidad de Buenos Aires, Buenos
529 Aires). Available from [[https://catalogo.exactas.uba.ar/cgi-bin/koha/opac-](https://catalogo.exactas.uba.ar/cgi-bin/koha/opac-detail.pl?biblionumber=49521)
530 [detail.pl?biblionumber=49521](https://catalogo.exactas.uba.ar/cgi-bin/koha/opac-detail.pl?biblionumber=49521)]

531 Bedoya Agudelo, E. L., Olivero, E., Concheyro, A., Torres Carbonell, P., & Martinioni,
532 D. (2018). Calcareous Nannofossils From La Barca Formation (Paleocene/Eocene
533 Boundary), Tierra Del Fuego, Argentina. *Ameghiniana*, 55(2), 2232–29.

534 Biddle, K. T., Uliana, M. A., Mitchum, R. M. Jr., Fitzgerald, M., & Wright, R. C.
535 (1986). The stratigraphic and structural evolution of the central and eastern
536 Magallanes Basin, southern South America. In P. A. Allen & P. Homewood (Eds.),
537 *Foreland basins* (pp. 41–61). International Association of Sedimentologists, Special
538 Publication.

539 Bown, P.R. & Young, J.R. (1998). Introduction. In P.R. Bown (Ed.), *Calcareous*
540 *Nannofossil Biostratigraphy* (pp. 1-15). Kluwer Academic, Dordrecht.

541 Bown, P. R. (2005). Palaeogene calcareous nannofossils from the Kilwa and Lindi areas
542 of coastal Tanzania (Tanzania Drilling Project 2003-4). *Journal of Nannoplankton*
543 *Research*, 27(1), 21–95.

544 Bown, P. R. (2016). Paleocene calcareous nannofossils from Tanzania. *Journal of*
545 *Nannoplankton Research*, 36(1), 1–32.

546 Flores, M. A., Malumián, N., Masiuk, V., & Riggi, J. (1973). Estratigrafía cretácica del
547 subsuelo de Tierra del Fuego. *Revista de La Asociacion Geologica Argentina*, 28,
548 407–437.

549 Furque, G., & Camacho, H. H. (1949). El Cretácico Superior de la costa Atlántica de
550 Tierra del Fuego. *Revista de La Asociación Geológica Argentina*, 4, 263–297.

- 551 Malumián, N. (1999). La sedimentación en la Patagonia extraandina. In R. Caminos
552 (Ed.), *Geología Argentina* (pp. 557–612). Anales del Servicio Geológico Minero
553 Argentino 29.
- 554 Malumián, N. (2002). El Terciario marino. Sus relaciones con el eustatismo. In M. J.
555 Haller (Ed.), *Geología y Recursos Naturales de Santa Cruz. Relatorio XV Congreso*
556 *Geológico Argentino. Asociación Geológica Argentina* (pp. 237–244). Buenos Aires.
- 557 Malumián, N. (1990). Foraminíferos bentónicos del Cretácico de cuenca Austral.
558 Argentina. In W. Volkheimer (Ed.), *Bioestratigrafía de los Sistemas Regionales del*
559 *Jurásico y Cretácico de América del Sur. Comité Sudamericano del Jurásico y*
560 *Cretácico* (pp. 429–495).
- 561 Malumián, N., & Caramés, A. (2002). Foraminíferos de sedimentitas ricas en carbono
562 orgánico, Formación La Barca, Paleoceno superior, Tierra del Fuego, Argentina.
563 *Revista de La Asociación Geológica Argentina*, 57(3), 219–231.
- 564 Malumián, N., & Jannou, G. (2010). Los Andes Fueguinos: el registro
565 micropaleontológico de los mayores acontecimientos paleoceanográficos australes
566 del Campaniano al Mioceno. *Andean Geology*, 37(2), 345–374.
- 567 Malumián, N., Jannou, G., & Nañez, C. (2009). Serial Planktonic Foraminifera from the
568 Paleogene of the Tierra del Fuego Island, South America. *Journal of Foraminiferal*
569 *Research*, 39(4), 316–321.
- 570 Malumián, N., & Olivero, E. (2006). El Grupo Cabo Domingo, Tierra del Fuego:
571 bioestratigrafía, paleoambientes y acontecimientos del Eoceno-Mioceno marino.
572 *Revista de La Asociación Geológica Argentina*, 61(2), 139–160.
- 573 Marensi, S., Casadío, S., & Santillana, S. (2002). La Formación Man Aike al sur de El
574 Calafate (Provincia de Santa Cruz) y su relación con la discordancia del Eoceno

575 medio en la cuenca Austral. *Revista de La Asociacion Geologica Argentina*, 57, 341–
576 344.

577 Martini, E. (1971). Standard Tertiary and Quaternary calcareous nannoplankton
578 zonation. In A. Farinacci (Ed.), *Proceedings of the II Planktonic Conference Roma*
579 (2nd ed., pp. 739-785). Edizioni Tecnoscienza.

580 Masiuk, V., Riggi, J. C., & Bianchi, J. L. (1990). Análisis geológico del Terciario del
581 subsuelo de Tierra del Fuego. *Boletín de Informaciones Petroleras*, 21, 70–89.

582 Mostajo, E. L. (1991). Nanofósiles calcáreos cenozoicos del Pozo “Las Violetas 3” Isla
583 Grande de Tierra del Fuego, Argentina. *Ameghiniana*, 28, 311–315.

584 Olivero, E. B., & Malumián, N. (2008). Mesozoic-Cenozoic stratigraphy of the Fuegian
585 Andes, Argentina. *Geologica Acta*, 16(1), 5–18.

586 Olivero, E. B., Malumián, N., & Martinioni, D. R. (2007). *Mapa geológico de la Isla*
587 *Gande de Tierra del Fuego e Islas de los Estados a escala 1: 500.000*. Servicio
588 Geológico Minero Argentino (SEGEMAR).

589 Olivero, E. B., Malumián, N., & Palamarczuk, S. (2003). Estratigrafía del Cretácico
590 Superior-Paleoceno del área de Bahía Thetis, Andes Fueguinos, Argentina:
591 Acontecimientos tectónicos y paleobiológicos. *Revista Geológica de Chile*, 30(2),
592 245–263.

593 Olivero, E. B., Malumián, N., Palamarczuk, S., & Scasso, R. A. (2002). El Cretácico
594 superior-Paleogeno del área del Río Bueno, costa atlántica de la Isla Grande de
595 Tierra del Fuego. *Revista de La Asociación Geológica Argentina*, 57(3), 199–218.

596 Olivero, E.B., Torres Carbonell, P.J., Svojtka, M., Fanning, M., Hervé, F., Nývlt, D.
597 (2020). Eocene volcanism in the Fuegian Andes: Evidence from petrography and
598 detrital zircons in marine volcanoclastic sandstones. *Journal of South American Earth*
599 *Sciences*, 104. <https://doi.org/10.1016/j.jsames.2020.102853>.

600 Perch-Nielsen, K. (1985). Cenozoic calcareous nannofossils. In K. Bolli, H.M.,
601 Saunders, J.B., Perch-Nielsen (Ed.), *Plankton Stratigraphy* (pp. 427–554).
602 Cambridge University Press.

603 Pérez Panera, J. P. (2009). Nanofósiles calcáreos paleógenos del sudeste de la provincia
604 de Santa Cruz, Patagonia, Argentina. *Ameghiniana*, 46(2), 273–284.

605 Pérez Panera, J. P. (2013). Paleogene calcareous nannofossil biostratigraphy for two
606 boreholes in the eastern Austral Basin, Patagonia, Argentina. *Andean Geology*, 40(1),
607 117–140.

608 Pérez Panera, J. P., Cuciniello, C. D., Bedoya Agudelo, É., & Olivero, E. B. (2017).
609 Early Eocene calcareous nannofossils of the Punta Torcida Formation, Austral Basin,
610 Patagonia: Biostratigraphy and Paleoceanography. *Journal of Nannoplankton*
611 *Research*, 37, 128–129.

612 Quattrocchio, M. E. (2021). Late Paleocene–middle Eocene dinoflagellate cysts from
613 the La Barca Formation, Austral Basin, Argentina. *Palynology*, 45(3), 421–428.

614 Raffi, I., Backman, J., & Palike, H. (2005). Changes in calcareous nannofossil
615 assemblages across the Paleocene/Eocene transition from the paleo-equatorial Pacific
616 Ocean. *Palaeogeography, Palaeoclimatology, Palaeoecology*, 226, 93–126.

617 Romans, B. W., Fildani, A., Hubbard, S. M., Covault, J. A., Fosdick, J. C., & Graham,
618 S. A. (2011). Evolution of deep-water stratigraphic architecture, Magallanes Basin,
619 Chile. *Marine Petroleum Geology*, 28, 612–628.

620 Sánchez, A., Pavlishina, P., Godoy, E., Hervé, F., & Fanning, M. C. (2010). On the
621 presence of Upper Paleocene rocks in the foreland succession at Cabo Nariz, Tierra
622 del Fuego, Chile: geology and new palynological and U-Pb data. *Andean Geology*,
623 37(2), 413–432.

- 624 Schneider, L. J., Bralower, T. J., & Kump, L. R. (2011). Response of nanoplankton to
625 early Eocene ocean destratification. *Palaeogeography, Palaeoclimatology,*
626 *Palaeoecology*, 310(3–4), 152–162.
- 627 Shamrock, J. L., & Watkins, D. K. (2012). Eocene calcareous nannofossil
628 biostratigraphy and community structure from Exmouth Plateau, Eastern Indian
629 Ocean (ODP Site 762). *Stratigraphy*, 9(1), 1–54.
- 630 Shepherd, C. L., & Kulhanek, D. K. (2016). Eocene nannofossil biostratigraphy of the
631 mid-Waipara River section, Canterbury Basin, New Zealand. *Journal of*
632 *Nannoplankton Research*, 36(1), 33–59.
- 633 Speijer, R., Pälke, H., Hollis, C., Hooker, J., & Ogg, J. (2020). The Paleogene Period.
634 In F. Gradstein, J. Ogg, M. Schmitz, G. Ogg (Eds.), *Geologic Time Scale 2020*, 1,
635 (pp. 1087–1140). Elsevier.
- 636 Thissen, J. M., & Pérez Panera, J. P. (2021). Cenozoic microfossil (Foraminifera and
637 calcareous nannofossils) assemblages from the subsurface Magallanes Basin, Tierra
638 del Fuego Island, Chile. *Publicación Electrónica de La Asociación Paleontológica*
639 *Argentina*, 21(1), 44–106.
- 640 Torres Carbonell, P. (2010). *Control tectónico en la estratigrafía y sedimentología de*
641 *secuencias sinorogénicas del Cretácico Superior-Paleógeno de la faja corrida y*
642 *plegada Fueguina*. (Tesis Doctoral, Departamento de Geología, Universidad
643 Nacional del Sur, Bahía Blanca).
- 644 Torres Carbonell, P. J., Dimieri, L.V., & Olivero, E. B. (2011). Progressive deformation
645 of a Coulomb thrust wedge: the eastern Fuegian Andes Thrust-Fold Belt. *Geological*
646 *Society, London, Special Publications*, 349(1), 123–147.

647 Torres Carbonell, P. J., Malumián, N., & Olivero, E. B. (2009). El Paleoceno-Mioceno
648 de Península Mitre: antefosa y depocentro de techo de cuña de la cuenca Austral,
649 Tierra del Fuego, Argentina. *Andean Geology*, 36(2), 197–235.

650 Torres Carbonell, P. J., & Olivero, E. B. (2019). Tectonic control on the evolution of
651 depositional systems in a fossil, marine foreland basin: Example from the SE Austral
652 Basin, Tierra del Fuego, Argentina. *Marine and Petroleum Geology*, 104, 40–60.

653 Young, J. R., Bown, P. R., & Lees, J. A. (2022). Nannotax3 website. *International*
654 *Nannoplankton Association*. <https://www.mikrotax.org/Nannotax3>.

655 **Figure captions**

656 **Figure 1. 1**, Location map and geological sketch of southeastern Tierra del Fuego. The
657 main stratigraphic units of the Southern Andes are shown. **2**, Geological map of the Río
658 Bueno area and location of the Río Claro Group and Río Bueno Formation sections.

659 **Figure 2**, Chronostratigraphic chart and correlation of Paleogene formations within the
660 different parts of the Austral Basin and coeval structural stages. Modified from Torres
661 Carbonell & Olivero (2019). Ages sources: **1**, Flores *et al.* (1973); Malumián (1990);
662 Masiuk *et al.* (1990); **2**, Malumián (1990, 2002); **3**, Olivero and Malumián (2008);
663 Torres Carbonell *et al.* (2009); **4**, Biddle *et al.* (1986); Sánchez *et al.* (2010); **5**,
664 Marensi *et al.* (2002); Romans *et al.* (2011). UC, Upper Cretaceous; **U1**, Unconformity
665 1; **U3**, Unconformity 3; **U4**, Unconformity 4.

666 **Figure 3. 1**, Composite profile including partial sections from different locations of the
667 Río Claro Group and Río Bueno Formation. After Olivero *et al.* (2002); **2**, LB2 member
668 of the La Barca Formation stratigraphic profile at the Punta Ainol area; **3**, LB1 member
669 of the La Barca Formation stratigraphic profile at the Río Malengüena area. Modified
670 from Bedoya Agudelo *et al.* (2018).

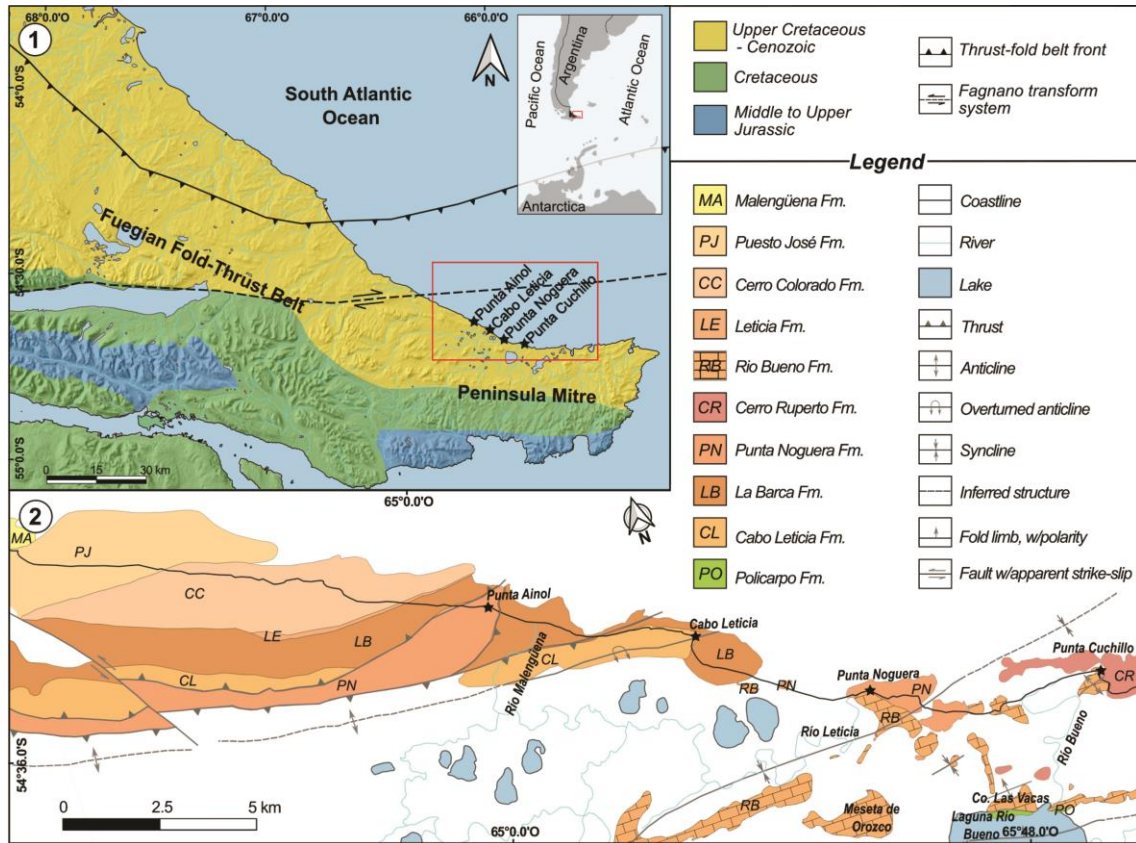
671 **Figure 4**, Stratigraphic distribution summary of calcareous nannofossils from the Río
672 Claro Group and the Río Bueno Formation, Tierra del Fuego, Austral basin.

673 **Figure 5**, Selected calcareous nannofossils recovered from the Río Claro Group and the
674 Río Bueno Formation; **1**, *Blackites* sp.; **2**, *Blackites spinosus*; **3**, *Braarudosphaera*
675 *bigelowii*; **4**, *Chiasmolithus bidens*; **5**, *Chiasmolithus grandis*; **6**, *Chiasmolithus nitidus*;
676 **7**, *Chiasmolithus solitus*; **8**, *Coccolithus formosus*; **9**, *Coccolithus latus*; **10**, *Coccolithus*
677 *pelagicus*; **11**, *Cyclicargolithus floridanus*; **12**, *Ellipsolithus bollii*; **13**, *Ericsonia*
678 *staerkeri*; **14**, *Fasciculithus involutus*; **15**, *Fasciculithus richardii*; **16**, *Fasciculithus*
679 *tyimpaniformis*; **17**, *Hornibrookina arca*; **18**, *Hornibrookina australis*; **19**, *Markalius*
680 *inversus*; **20**, *Neochiastozygus concinnus*. Cerro Ruperto Formation (1,4,8,9,10,11,12);
681 La Barca Formation (14, 15, 16, 17,18, 19, 20); Punta Noguera (6,3); Río Bueno (
682 2,5,7,13). Scale bar equals 5 µm.

683 **Figure 6**, Selected calcareous nannofossils recovered from the Río Claro Group and the
684 Río Bueno Formation; **1**, *Neochiastozygus junctus*; **2**, *Neococcolithes dubius*; **3**,
685 *Neococcolithes minutus*; **4**, *Pontosphaera exilis*; **5**, *Pontosphaera pectinata*; **6**,
686 *Pontosphaera pulchra*; **7**, *Prinsius bisulcus*; **8**, *Rhomboaster cuspis*; **9**, *Toweius*
687 *callosus*; **10**, *Toweius eminens*; **11**, *Toweius occultatus*; **12**, *Toweius tovae*; **13**,
688 *Reticulofenestra dictyoda*; **14**, *Reticulofenestra lockeri*; **15**, *Reticulofenestra minuta*; **16**,
689 *Reticulofenestra wadeae*. Cerro Ruperto Formation (5,6,13,14,15); La Barca Formation
690 (7,8,10,11,12); Punta Noguera (1); Río Bueno (2,3,4,9,16). Scale bar equals 5 µm.

691 **Figure 7**, Calcareous nannofossil assemblages recognized in surface and subsurface of
692 Paleogene lithostratigraphic units in the Austral Basin, their correspondence with the
693 biozones of Martini (1971) and considering the ages they represent. Correlation with
694 other known microfossil assemblages (foraminifera and/or dinocyst). References: **1**,
695 Bedoya Agudelo *et al.* (2018); **2**, Bedoya Agudelo (2019); **3**. This work; **4**, Mostajo

696 (1991); **5**, Thissen and Pérez Panera (2021); **6**, Pérez Panera (2009); **7**, Pérez Panera
 697 (2013); **8**, Olivero *et al.* (2002); **9**, Malumián *et al.* (2009); **10**, Torres Carbonell *et al.*
 698 (2009); **11**, Malumián and Jannou (2010); **12**, Quattrocchio (2021).

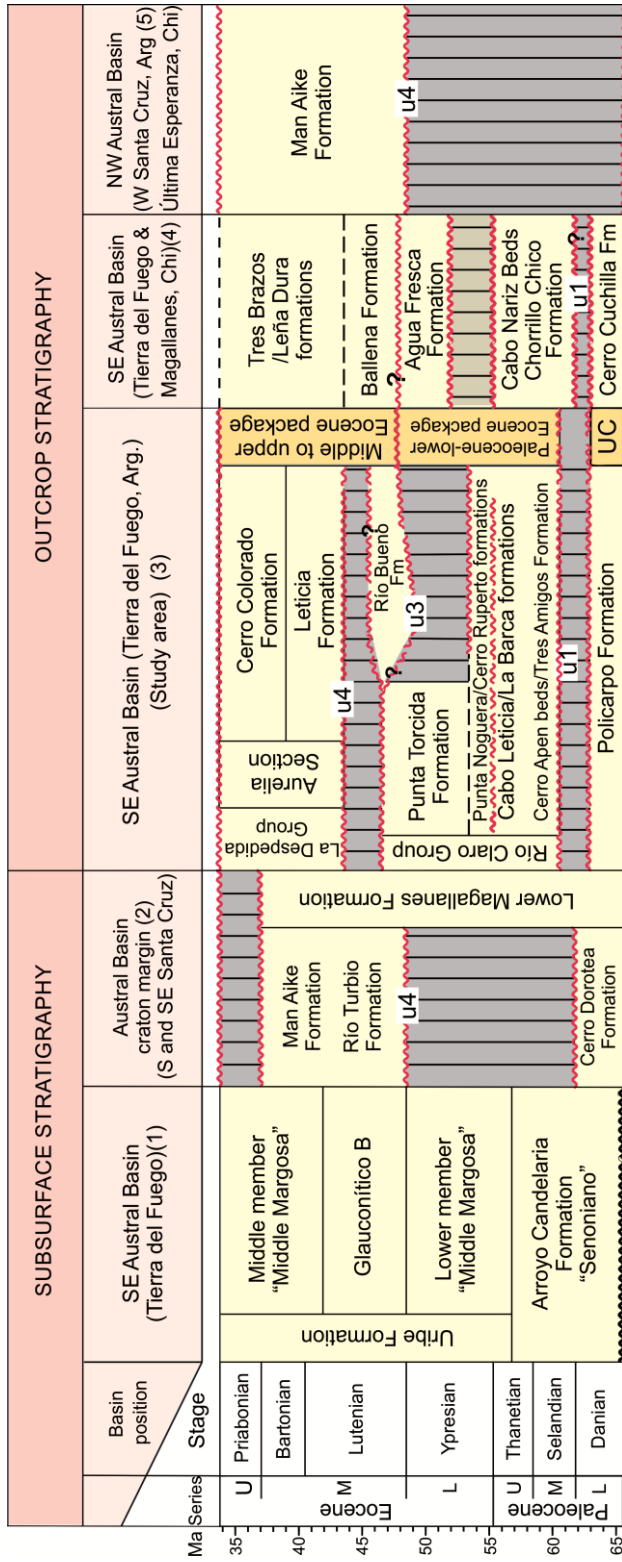


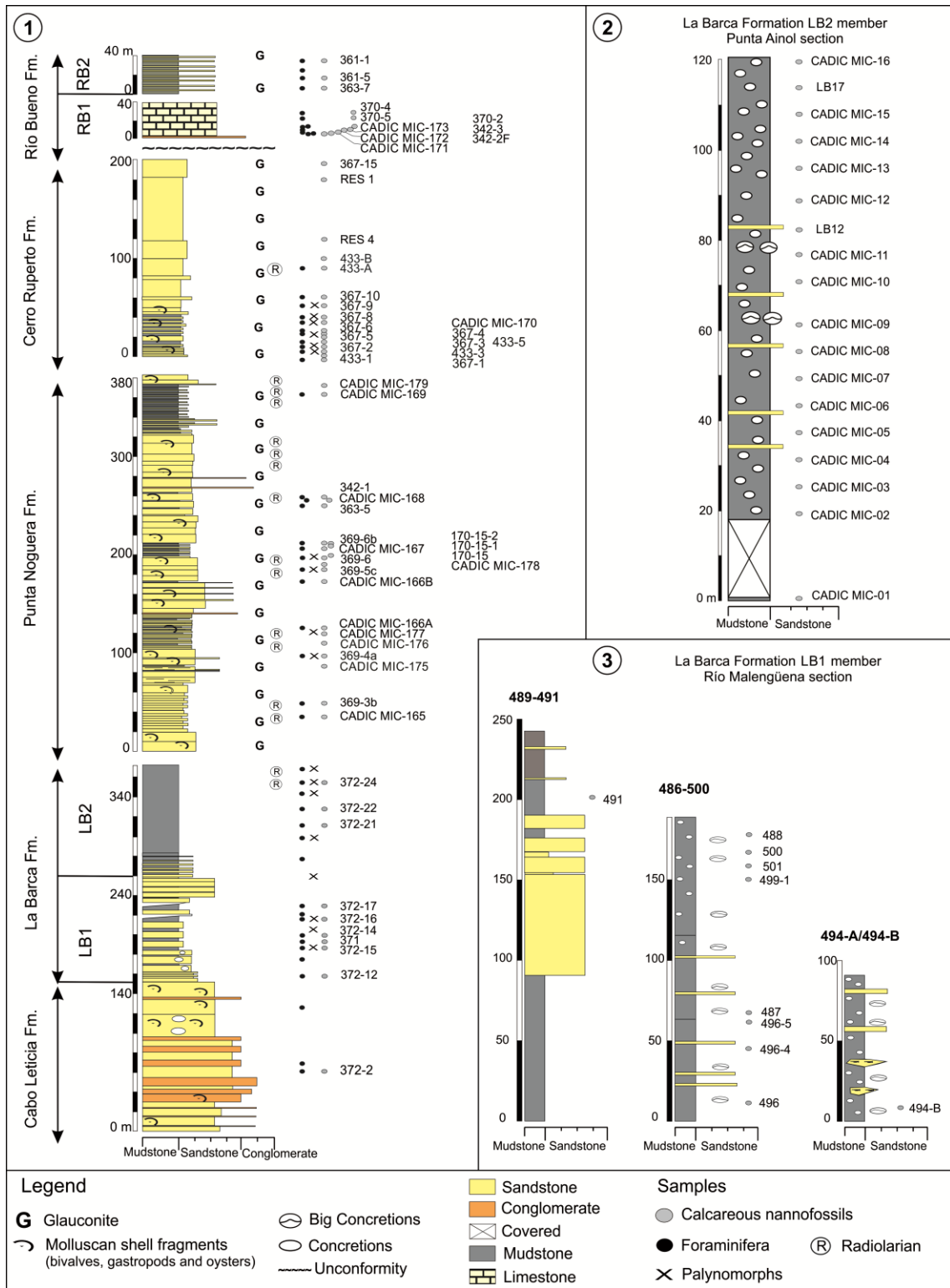
699

700 Figure 1.

701

702 Figure 2.





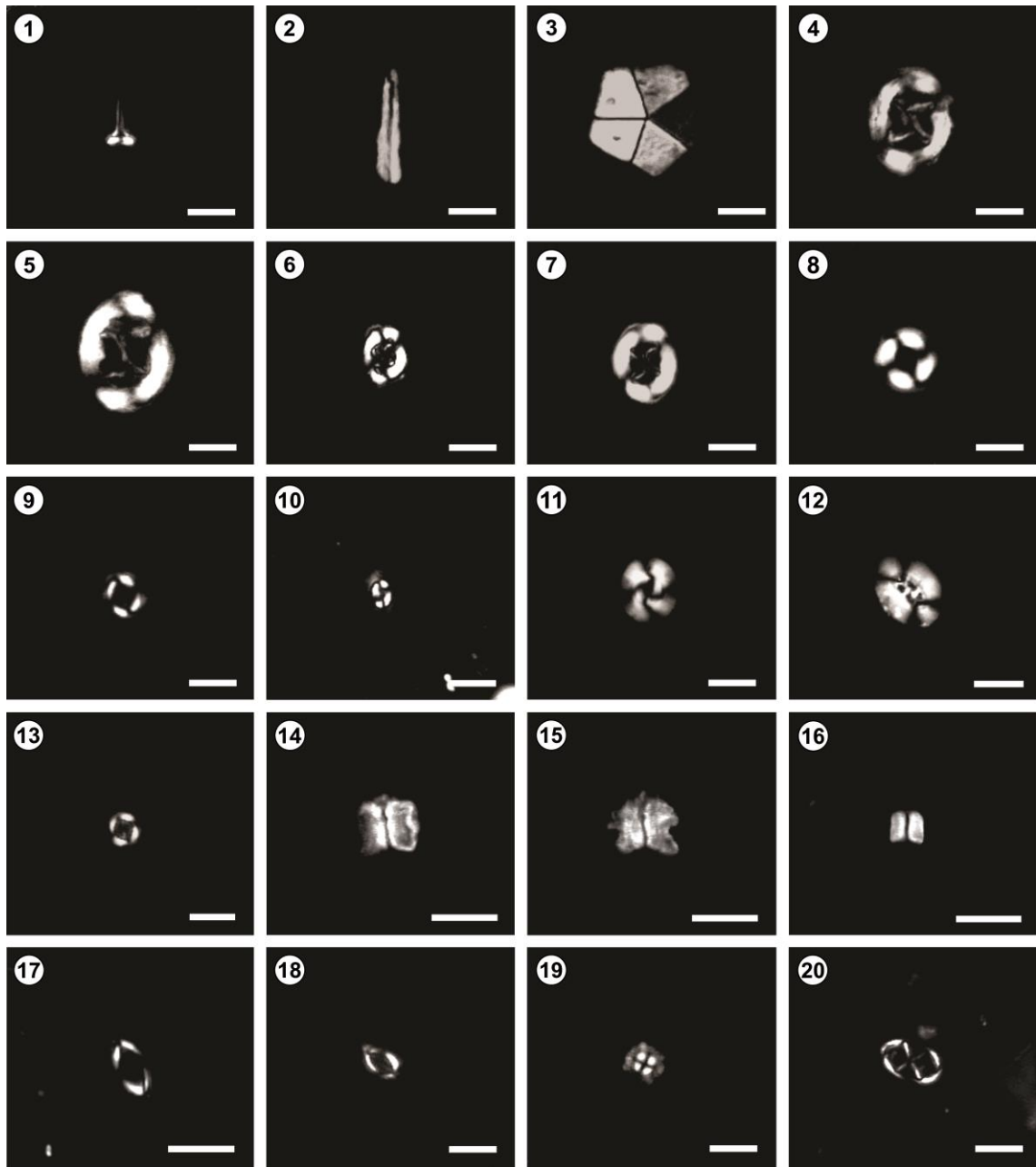
703

704 Figure 3.

Taxa	Formation	La Barca	Punta Noguera	Cerro Ruperto	Río Bueno
<i>Blackites</i> sp.			*		
<i>Blackites</i> cf. <i>creber</i>				*	
<i>Braarudosphaera bigelowii</i>		*	*		*
<i>Chiasmolithus bidens</i>		*	*		*
<i>Chiasmolithus eograndis</i>		*	*		*
<i>Chiasmolithus expansus</i>					*
<i>Chiasmolithus modestus</i>				*	
<i>Chiasmolithus nitidus</i>		*	*		
<i>Chiasmolithus solitus</i>		*	*	*	*
<i>Coccolithus formosus</i>				*	
<i>Coccolithus latus</i>				*	
<i>Coccolithus pelagicus</i>		*	*	*	*
<i>Coccolithus</i> cf. <i>crasus</i>				*	
<i>Coronocyclus bramlettei</i>				*	
<i>Cyclicargolithus luminis</i>					*
<i>Cyclicargolithus parvus</i>			*		
<i>Dictyococcites productus</i>				*	
<i>Discoaster</i> cf. <i>araneus</i>		*			
<i>Ellipsolithus bollii</i>				*	*
<i>Ericsonia staerkeri</i>					*
<i>Ericsonia subpertusa</i>		*	*		
<i>Fasciculithus</i> cf. <i>alanii</i>		*	*		
<i>Fasciculithus involutus</i>		*	*		
<i>Fasciculithus</i> cf. <i>mitreus</i>		*	*		
<i>Fasciculithus richardii</i>		*	*		
<i>Fasciculithus</i> cf. <i>sidereus</i>			*		
<i>Fasciculithus tympaniformis</i>		*	*		
<i>Helicosphaera lophota</i>		*	*		
<i>Helicosphaera</i> spp.		*	*	*	*
<i>Helodiscolithus solidus</i>		*	*		
<i>Hornibrookina arca</i>		*	*		*
<i>Hornibrookina australis</i>		*	*		
<i>Lanternithus duocavus</i>			*		
<i>Lanternithus simplex</i>		*	*		
<i>Lanternithus unicavus</i>			*		
<i>Markalius inversus</i>			*		*
<i>Neochiastozygus concinnus</i>		*	*		*
<i>Neochiastozygus junctus</i>		*	*		*
<i>Neococcolithes dubius</i>			*	*	*
<i>Neococcolithes minutus</i>					*
<i>Neococcolithes protenus</i>		*			*
<i>Pontosphaera duocava</i>					*
<i>Pontosphaera exilis</i>		*			*
<i>Pontosphaera pectinata</i>				*	
<i>Pontosphaera plana</i>					*
<i>Pontosphaera pulchra</i>			*	*	*
<i>Pontosphaera versa</i>					*
<i>Prinsius bisulcus</i>		*	*		
<i>Prinsius martini</i>			*		
<i>Reticulofenestra dictyoda</i>				*	
<i>Reticulofenestra lockeri</i>				*	
<i>Reticulofenestra minuta</i>				*	
<i>Reticulofenestra producta</i>				*	
<i>Reticulofenestra</i> spp.				*	*
<i>Reticulofenestra wad eae</i>					*
<i>Rhomboaster cuspis</i>		*			
<i>Sphenolithus moriformis</i>		*			*
<i>Sphenolithus</i> spp.		*		*	*
<i>Thoracosphaera</i> spp.		*	*		
<i>Toweius callosus</i>			*	*	*
<i>Toweius eminens</i>		*	*		
<i>Toweius gammaton</i>					*
<i>Toweius occultatus</i>		*	*	*	*
<i>Toweius pertusus</i>		*			
<i>Toweius rotundus</i>		*			
<i>Toweius serotinus</i>		*			
<i>Toweius</i> spp.		*	*	*	*
<i>Toweius tovae</i>		*			*
<i>Umbilicosphaera</i> spp.		*			*
<i>Zygrhablithus bijugatus</i>		*	*		*

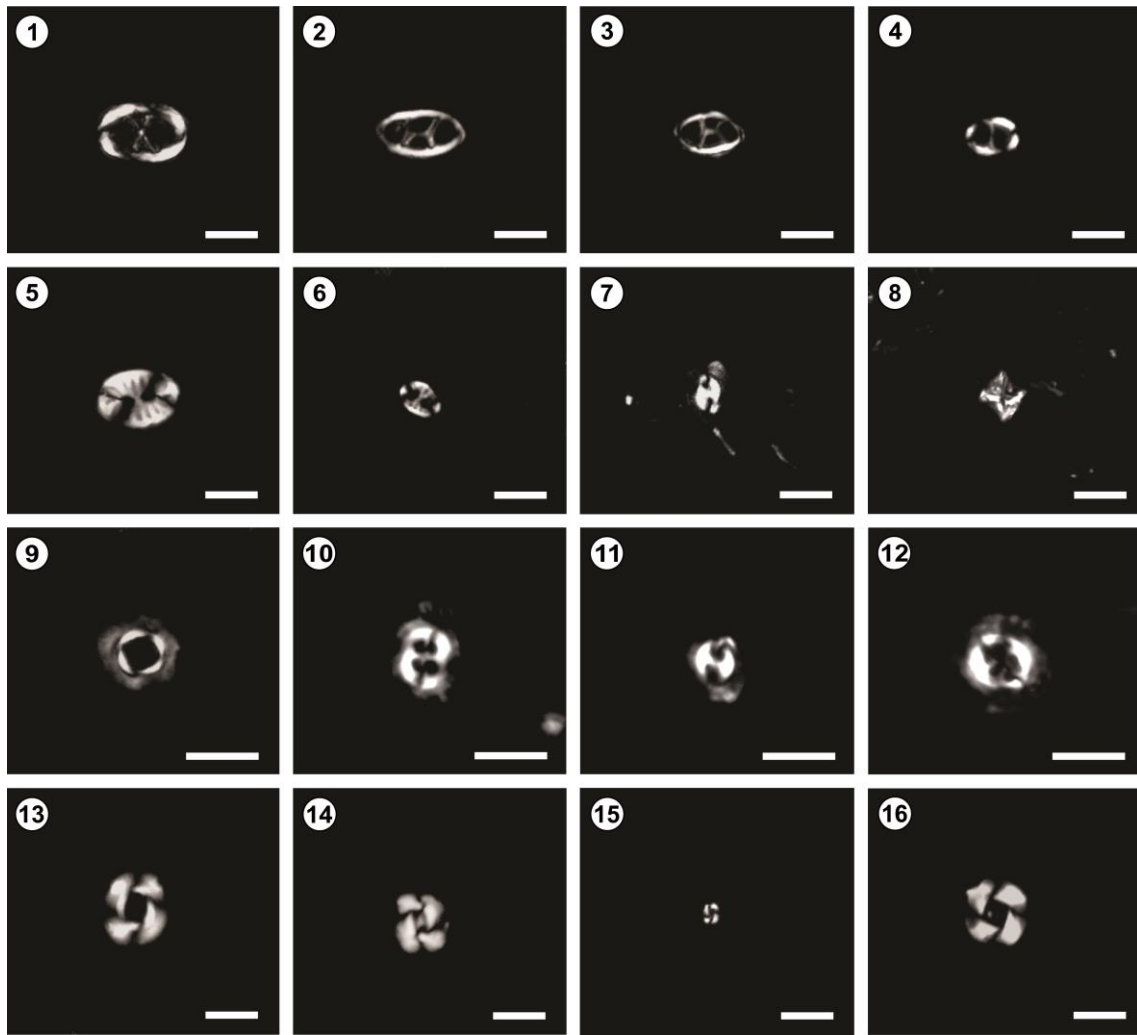
705

706 Figure 4.



707

708 Figure 5.



709

710 Figure 6.

Formation	Member	Age	Calcareous Nannofossil Zone (Martini, 1971)	Calcareous Nannofossil assemblage outcrop (1,2,3)	Calcareous Nannofossil assemblage subsurface		Microfossil assemblage outcrop (8,9,10,11,12)	
					SE Austral basin Tierra del Fuego (4,5)	Austral basin Santa Cruz (6 7)	Foraminifera	Dinocysts
Río Bueno	RB1	early Eocene middle Eocene	NP14-NP15	<i>Chiasmolithus grandis</i> <i>Chiasmolithus solitus</i> <i>Chiasmolithus expansus</i> <i>Reticulofenestra wadeae</i> <i>Neococcolithes minutus</i>	<i>B. bigelowii</i> <i>C. consuetus</i> <i>C. expansus</i> <i>N. dubius</i> <i>Z. bijugatus</i>	<i>C. modestus</i> <i>C. solitus</i> <i>P. multipora</i> <i>P. pulchra</i> <i>R. daviessi</i> <i>R. dictyoda</i> <i>R. minuta</i> <i>R. scrippsae</i>	<i>Planorotalites australiformis</i> <i>Subbotina linaperta</i> <i>Subbotina patagonica</i>	
	RB2			<i>Reticulofenestra</i> spp. <i>Toweius callosus</i> <i>Zygrhablithus bijugatus</i>				
Cerro Ruperto		early Eocene	NP12-NP13	<i>Coccolithus formosus</i> <i>Neococcolithes dubius</i> <i>Reticulofenestra dictyoda</i> <i>Toweius callosus</i>	<i>C. bidens</i> <i>C. consuetus</i> <i>C. solitus</i> <i>C. pelagicus</i> <i>E. distichus</i> <i>P. multipora</i> <i>P. pulchra</i> <i>T. gammatum</i> <i>Z. bijugatus</i>		<i>Spiroplectamina spectabilis</i>	<i>Deflandrea dartmoria</i> <i>Deflandrea antarctica</i>
Punta Noguera		early Eocene	NP9b-NP10	<i>Chiasmolithus bidens</i> <i>Chiasmolithus solitus</i> <i>Hornibrookina australis</i> <i>Fasciculithus involutus</i> <i>Fasciculithus tympaniformis</i> <i>Prinsius martini</i> <i>Rhomboaster cuspis</i> <i>Toweius eminens</i> <i>Toweius pertusus</i>	<i>C. bidens</i> <i>C. consuetus</i> <i>C. solitus</i> <i>C. pelagicus</i> <i>E. distichus</i> <i>P. multipora</i> <i>P. pulchra</i> <i>T. gammatum</i> <i>Z. bijugatus</i>	<i>C. bidens</i> <i>Fasciculithus tympaniformis</i> <i>P. martini</i> <i>T. callosus</i> <i>T. eminens</i> <i>T. pertusus</i>	<i>Chiloguembelina wilcoxensis</i> <i>Chiloguembelina noguerensis</i> <i>Rzehakina</i> <i>Cribrotalia</i> <i>Elphidium</i>	<i>Apectodinium homomorphum</i> <i>Deflandrea robusta</i> <i>Palaeocystodinium cf. golzowense</i>
La Barca	LB1	late Paleocene - early Eocene	NP9a-NP9b	—	—	—	<i>Bulimina karpatica</i> <i>Stensioeina beccariformis</i> <i>Spiroplectamina spectabilis</i> <i>Bulimina isabelleana</i> <i>procera</i> <i>Anctarticea</i> sp.	<i>Palaeocystodinium golzowense</i> <i>Glaphyrocysta</i>
	LB2			<i>Chiasmolithus bidens</i> <i>Discoaster</i> cf. <i>araneus</i> <i>Ericsonia subpertusa</i> <i>Hornibrookina australis</i> <i>Fasciculithus alanii</i> <i>Fasciculithus mitreus</i> <i>Fasciculithus richardii</i> <i>Fasciculithus tympaniformis</i> <i>Prinsius bisulcus</i> <i>Rhomboaster cuspis</i> <i>Toweius serotinus</i>			<i>Apectodinium homomorphum</i> <i>Cleistosphaeridium diversispinosum</i> <i>Enneadocysta dictyostila</i> <i>Impagidium crassimuratum</i> <i>Samlandia septata</i>	
Cabo Leticia		late Paleoc.	—	—	—	—	—	—

711

712 Figure 7.

TABLE 1. Sampling summary of the Río Claro Group and the Río Bueno Formation

Formation	Samples with profile associated	Isolated samples	Fertile samples	Barren samples	Sample Code Repository (Barren samples without code)	Total samples analyzed
Cabo Leticia	1	1	—	2	—	2
La Barca	38	0	22	16	CADIC MIC-01 to 16	38
Punta Noguera	21	0	10	11	CADIC-MIC 165 to 169; CADIC MIC-175 to 179	21
Cerro Ruperto	17	0	1	17	CADIC-MIC 170	18
Río Bueno	11	5	4	12	CADIC-MIC 171 to 174	16

713